Proc. NIPR Symp. Polar Meteorol. Glaciol., **6**, 1–15, 1992

ESTIMATION OF SURFACE ALBEDO DISTRIBUTION IN LÜTZOW-HOLM BAY AND ITS NEIGHBORHOOD WITH NOAA/AVHRR DATA

Kiyotaka NAKAGAWA

Division of Science, Joetsu University of Education, Yamayashikimachi 1, Joetsu 943

Abstract: A method has been developed for estimating the filtered narrow band surface albedo with NOAA/AVHRR data, and has been applied to analysis of the surface albedo distribution in Lützow-Holm Bay and its neighborhood, Antarctica, in 1990. As a result, 16 maps of the surface albedo distribution have been drawn. From a comparison of the albedos inferred from satellite data with those actually observed in Ongul Strait, it is clear that the satellite-inferred, filtered narrow band albedos agree well with the daily means of ground-observed, unfiltered broad band albedo, despite systematic errors of about −4 %. It is also clear that there is a characteristic pattern of surface albedo distribution in this area; the open sea has very low albedo of less than 5 %, whereas most of the compact pack ice and fast ice has high albedo of more than 60 %. The albedo is lower in the eastern part of Lützow-Holm Bay than in the western part; especially off the Sôya Coast it is less than 40 %. The ice sheet of Antarctica has remarkably high albedo of more than 80 %.

1. Introduction

The advanced very high resolution radiometer on board the NOAA polar orbiting satellite (NOAA/AVHRR) is a scanning radiometer which has five channels (numbered 1–5) in the visible, near infrared, reflected infrared, and thermal, emitted infrared portions of the electromagnetic spectrum (1 : 0.58–0.68 μm, 2 : 0.725–1.10 μm, 3 : 3.55–3.93 μm, 4 : 10.3–11.3 μm, 5 : 11.5–12.5 μm). Its resolution at the satellite subpoint is 1.1 km. The NOAA satellite data have been received at Syowa Station (69°00′S, 39°35′E) continuously since the 21st Japanese Antarctic Research Expedition (JARE-21) in 1980. Especially under the "Antarctic Climate Research (ACR)" project, which started in 1987, a NOAA/AVHRR data processing system with a FACOM S-3300 mini computer was installed to acquire the received satellite data in real time, to convert raw data to reflectances (Channels 1 and 2) or equivalent black body temperatures (Channels 3, 4 and 5), to make map projections, to display the images, and to store the data on computer compatible tapes (CCT). The operation has been done once a day for the northward path in which the NOAA satellite elevation angle is the highest on that day.

The main purposes of receiving NOAA/AVHRR data at Syowa Station are to obtain information about clouds, ice sheet and sea ice over the Antarctic region. The temporal and geographical distributions of the surface albedo over

this area are among the most required information. The author passed the 1990 winter at Syowa Station as one of the members of the winter party of JARE-31, and engaged both in receiving the NOAA satellite data and in observing micrometeorological conditions over the sea ice in Ongul Strait near the station.

The purpose of the present study is to develop a method for estimating the surface albedo with NOAA/AVHRR data, and to analyze the surface albedo distribution in Lützow-Holm Bay and its neighborhood. To infer surface albedo from satellite data, different methods are presently used (*e.g.* OTTERMAN and FRASER, 1976; ROCKWOOD and COX, 1978; MEKLER and JOSEPH, 1983; CHEN and OHRING, 1984). The method developed here is a modification of CHEN and OHRING's (1984) method.

2. Method for Estimating Surface Albedos from NOAA/AVHRR Data

There are many difficulties in the use of the NOAA/AVHRR data for study of surface albedo, such as the anisotropy of the reflected solar radiation field at the top of the atmosphere, the scatter and absorption of radiation through the atmosphere lying between the ground and the satellite, the selective spectral response of the sensor, and so on. However, the present study, according to GRUBER (1977) and GRUBER *et al.* (1983), assumes that reflectance is not dependent on zenith and azimuth angles, and that the ground reflectivity is not dependent on the solar zenith angle, since well-defined angular models are not yet available for the reflected solar radiation at the top of the atmosphere; and LACIS and HANSEN's (1974) parameterization, which is applied by the present study, also uses this approximation. In addition, the present study deals with the spectral range of NOAA/AVHRR Channels 1 and 2, *i.e.* 0.58–0.68 μm and 0.725–1.1 μm. In other words, the surface albedo inferred in the present study is also for this narrow spectral region.

First, we have to obtain the filtered planetary albedo in the wavelength region of NOAA/AVHRR Chaneels 1 and 2. Since the ratio of spectral solar constants between both wavelength regions 0.58–0.68 μm and 0.725–1.1 μm is 0.317 : 0.683 (THEKAEKARA and DRUMMOND, 1971), the filtered planetary albedo in the wavelength region of NOAA/AVHRR Channels 1 and 2, A_p, can be obtained by the following formula:

$$A_p=(0.317A_1+0.683A_2)\,[1+0.0167\sin\{2\pi\,(J-93.5)\,/\,365\}]^2\,/\,\mu. \qquad (1)$$

Here, μ is the cosine of the solar zenith angle; and A_1 and A_2 are, respectively, filtered reflectances in the wavelength regions of NOAA/AVHRR Channels 1 and 2, which are given by the NOAA/AVHRR data processing system of Syowa Station. The term in square brackets in eq. (1) is the correction for the distance between the sun and earth (GURNEY and HALL, 1983), and J is Julian day.

Next, we have to make the atmospheric correction in order to obtain the surface albedo from the planetary albedo. In the present study the atmospheric correction is done by modifying CHEN and OHRING's (1984) method, which is based upon LACIS and HANSEN's (1974) parameterization. According to their

parameterization, the major absorbers in the earth–atmosphere system are ozone in the stratosphere, water vapor in the troposphere and the earth's surface, the absorptances of which are functions of the water vapor and ozone distribution, the zenith angle of the sun and the albedo of the earth's surface. Their parameterization divides the absorption by the above absorbers into two parts, one for the wavelength region longer than 0.7 μm where water absorption is significant and one for the remaining wavelengths where ozone absorption is significant, and takes Rayleigh scattering into account in the spectral region of negligible water vapor absorption. Since the above absorptances and Rayleigh scattering are expressed in units of the total solar constant, we can obtain the planetary albedo by subtracting the sum of these absorptances from unity, as shown by CHEN and OHRING (1984). However, LACIS and HANSEN's (1974) parameterization can not be applied directly to the NOAA/AVHRR data, since it has been proposed for unfiltered solar radiation. It is necessary to convert this parameterization from unfiltered spectral range to the filtered range of NOAA/AVHRR Channels 1 and 2.

Although LACIS and HANSEN's (1974) parameterization expresses the ozone and water vapor absorptivities and the Rayleigh albedos in units of the total solar constant, they have to be converted to the expressions in units of the filtered solar constant in the wavelength region of NOAA/AVHRR Channels 1 and 2. According to THEKAEKARA and DRUMMOND (1971), the ratio of the filtered solar constant in the wavelength region of NOAA/AVHRR Channels 1 and 2 to the total solar constant is 0.367. Therefore, we can express such parameters in units of the filtered solar constant, dividing the original parameterization of LACIS and HANSEN (1974) by 0.367 after excluding the contributions outside of the wavelength region of NOAA/AVHRR Channels 1 and 2 from it.

Since the ratio of spectral solar constants between the spectral regions of NOAA/AVHRR Channels 1 and 2 is 0.317 : 0.683 as described above, the fraction of the filtered solar constant in the spectral region of NOAA/AVHRR Channels 1 and 2 absorbed at the earth's surface, A_s, is given by

$$A_s=\left\{\frac{0.317-R_r-A_o(x)}{1-R_r^* A_g}+0.683-A_w(y)\right\}(1-A_g), \tag{2}$$

where A_g is the filtered surface albedo, A_o and A_w are, respectively, the ozone and water vapor absorptivities, and x and y are the total atmospheric ozone and water vapor path lengths traversed by the direct solar beam in reaching the earth's surface, which are given by

$$x = uM, \tag{3}$$
$$y = wM. \tag{4}$$

Here, M $(=35/\sqrt{1224\mu^2+1})$ is the optical air mass, u is the total ozone amount (atm-cm), w is the effective water vapor content (cm), which is estimated from air temperature, T_0 (K), air pressure, p_0 (hPa), and water vapor pressure, e_0 (hPa), by the following formula (NAKAGAWA, 1988):

$$w=0.0351e_0\, p_0 / T_0. \tag{5}$$

Although eq. (5) has been derived from BRUTSAERT's (1975) approximation of vertical profiles on the lapse conditions, as shown in Fig. 1, it is indeed a good approximation even in the polar region. A_o is derived by dividing only half of the term for the Chappuis band of the original parameterization by 0.367. A_w is also derived by dividing the original parameterization by 0.367, after excluding the contributions of the wavelength region longer than 1.1 μm, using LIOU and SASAMORI's (1975) parameterization. R_r is the Rayleigh albedo of the total atmosphere for the incoming solar radiation flux, which, in parameterized form, is given by

$$R_r=0.050 / (1+6.43\,\mu), \tag{6}$$

and R_r^* (=0.0122) is the spherical albedo of the total atmosphere for the radiation from below.

The fraction of the filtered solar constant absorbed in the atmosphere, A_a, is given by

$$A_a=A_o\,(x)+\left\{R_a+\frac{(1-R_a)\,(1-R_a^*)A_g}{1-R_a^*A_g}\right\}\{A_o\,(x^*)-A_o\,(x)\}$$
$$+A_w\,(y)+A_g\,\{A_w\,(y^*)-A_w\,(y)\}, \tag{7}$$

where x^* and y^* are the total path lengths of, respectively, ozone and water vapor traversed by the reflected radiation in reaching the top of the atmosphere,

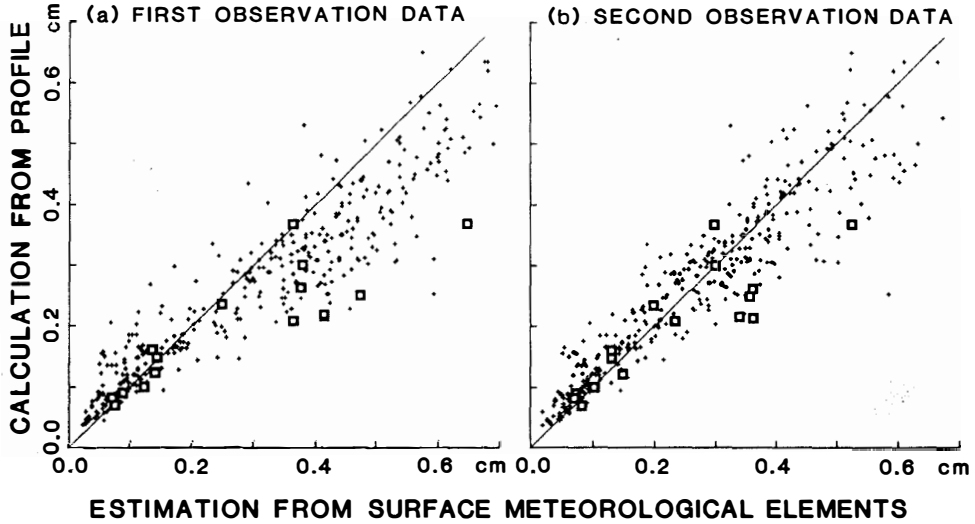

Fig. 1. Plot of the effective water vapor contents estimated by eq. (5) based upon the first (a) or second (b) data of radio sounding at Syowa Station versus that calculated from all the data of the ascending profile. The estimation from the second data measured at a few scores meters above the ground is better than that from first data measured at the surface before flying, probably due to the influence of the structure and/or observer. Open squares stand for days when the surface albedo is inferred in the present paper, and dots for other days during the period from February 1, 1990 to January 31, 1991.

R_a is the Rayleigh albedo of the atmosphere underlying the ozone layer for the incoming solar radiation flux, which, in parameterized form, are given by

$$x^* = u\,(M+1.9), \tag{8}$$
$$y^* = w\,(M+5/3), \tag{9}$$
$$R_a = 0.039 \,/\, (1+0.816\,\mu), \tag{10}$$

and R_a^* (=0.0256) is the spherical albedo of the atmosphere underlying the ozone layer for radiation from below.

Subtracting both A_s and A_a from unity, the relationship between the filtered planetary albedo, A_p, and the filtered surface albedo, A_g, is expressed as follows:

$$A_p=0.317-A_o\,(x)-R_a\{A_o\,(x^*)-A_o\,(x)\}-\frac{0.317-R_r-A_o\,(x)}{1-R_r^*A_g}+[0.683-A_w\,(y^*)$$
$$+\frac{0.317-R_r-A_o\,(x)}{1-R_r^*A_g}-\frac{(1-R_a)\,(1-R_a^*)}{1-R_a^*A_g}\{A_o\,(x^*)-A_o\,(x)\}]A_g. \tag{11}$$

With eq. (11), the filtered planetary albedo was simulated for a variety of filtered surface albedos, surface air temperatures, surface atmospheric pressures, surface water vapor pressures, total ozone amounts, and solar elevations. As a result, it was shown that the planetary albedo is mainly a linear function of the surface albedo, and is also relatively sensitive to the solar elevation and the surface water vapor pressure. Figure 2 shows an example of the relationship between the planetary and surface albedos, predicted by eq. (11) at every 0.05 surface albedo under the assumption that T_0=267.35 K, e_0=2.9 hPa, p_0=992.3 hPa, u=0.288 atm-cm, and the solar elevation is 16.0°, which are meteorological

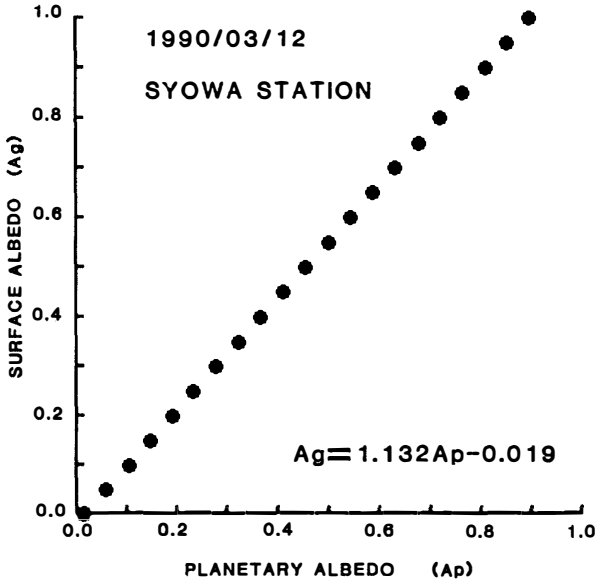

Fig. 2. The relationship between the planetary and surface albedos predicted by eq. (11) under the assumption that T_0=267.35 K, e_0=2.9 hPa, p_0=992.3 hPa, u=0.288 atm−cm, and the solar elevation is 16.0 °.

conditions for 1558 LST on 12 March 1990 at Syowa Station. The regression line is given by

$$A_g = 1.132A_p - 0.019, \quad (12)$$

with the determination factor of 0.9999. Then, if we can detect the filtered planetary albedo correctly from the NOAA/AVHRR data, we can easily determine the filtered surface albedo with the regression line. The regression line is determined separately for every pixel; the solar elevation is calculated based upon orbital elements, and the temperature of NOAA/AVHRR Channel 4 is regarded as the surface air temperature. The surface water vapor pressure is given from that temperature, assuming that it is saturated over the ice surface. The surface atmospheric pressure and total ozone amount are assumed to be the same as those at Syowa Station through the whole region.

3. Results

Table 1 shows the monthly path numbers of the NOAA 11 satellite received at Syowa Station by JARE-31. Data are missing on days when no path was received, chiefly due to an accident to a receiving antenna. Despite 18 missing data, we obtained CCT data for 402 paths in the whole year. Since most of them passed over Syowa Station between 1500 and 1700 LST, data from the middle of April to the beginning of September, in the polar night, were not available for the analysis of surface albedo distribution around Syowa Station. Therefore, the present study looked for the available paths from the data of the remaining period using the cloud detection method proposed by YAMANOUCHI *et al.* (1987), which has also been installed in the mini computer of Syowa Station.

As a result, the present study analyzed the surface albedo distribution for 16 samples, as shown in Table 2. Since there were almost always clouds near the fringe of the sea ice, it was difficult to find a completely cloud free scene over Lützow-Holm Bay and its neighborhood. Therefore, most of the 16 scenes selected above have a few cloud-contaminated pixels. But this does not affect the overall surface albedo distribution over this area.

Figure 3 shows an example of the distribution map of surface albedo in this area in autumn, analyzed for 1558 LST on 12 March 1990. This figure consists of 416 × 380 pixels, assigning each a gray scale value from black (0) to white (85);

Table 1. Numbers of NOAA11 paths received at Syowa Station by JARE-31.

Year	'90											'91	
Month	Feb.	Mar.	Apr.	May	June	July	Aug.	Sep.	Oct.	Nov.	Dec.	Jan.	Total
Received paths	33	33	38	38	29	33	32	39	35	33	33	26	402
Missing data	1	0	0	1	5	2	2	0	1	0	0	6	18
Analyzed paths	2	1	1	0	0	0	0	3	3	4	2	0	16

Table 2. Dates of analysis and values of parameters used here.

No.	Path ID	Date	Time	Satellite elevation degree	Solar elevation degree	Air pressure hPa	Ozone amount m-atm-cm
1	K07123	1990 / 02 / 11	1607	83.1	25.8	987.6	309
2	K07264	1990 / 02 / 21	1101	88.0	23.0	992.6	298
3	K07532	1990 / 03 / 12	1558	89.7	16.0	992.3	288
4	K07828	1990 / 04 / 02	1532	71.7	9.5	984.9	283
5	K10128	1990 / 09 / 12	1606	87.5	7.3	976.0	201
6	K10312	1990 / 09 / 25	1704	59.3	7.0	979.9	153
7	K10368	1990 / 09 / 29	1620	84.1	12.0	980.2	172
8	K10622	1990 / 10 / 17	1623	83.1	17.8	996.2	252
9	K10749	1990 / 10 / 26	1624	82.5	20.6	985.6	350
10	K10763	1990 / 10 / 27	1613	90.3	21.8	1000.1	344
11	K11073	1990 / 11 / 18	1530	60.7	31.4	1001,2	226
12	K11102	1990 / 11 / 20	1649	68.5	25.3	1000.6	241
13	K11116	1990 / 11 / 21	1638	75.0	26.5	996.1	305
14	K11130	1990 / 11 / 22	1627	83.0	27.7	991.1	323
15	K11313	1990 / 12 / 05	1543	68.2	33.8	978.8	289
16	K11610	1990 / 12 / 26	1651	68.6	29.8	989.8	317

isolines of albedos of 5, 40, 60 and 75 % are drawn. Lützow-Holm Bay is in the central part of the figure, with horizontal dimensions around 100 km × 300 km. The bay is perfectly covered with fast ice whose albedo is lower in the eastern part rather than in the western part. The albedo over fast ice is higher than 60 % except off the Sôya Coast where it is snow free over the ice surface, and the albedo is remarkably lower than 40 %. The albedo of the open sea in the Indian Ocean is less than 5 %, and the albedo of open pack ice is also low, *i.e.* less than 40 %. On the other hand, the Antarctic Continent has high albedo ranging from 80 to 114 %. However, since the effects of the elevation and slope of the ice sheet are not taken into account in the present study, the analyzed value over the Antarctic Continent in Fig. 3 is not the truly correct albedo; the analyzed albedo must be too high on sunny slopes, and too low on shady slopes. For example, the eastern coast of the Riiser-Larsen Peninsula, which is shady, has albedo less than 75 %, and some parts of the Prince Olav Coast or the Sôya Coast, which are sunny, have albedo more than 100 %.

Figure 4 shows an example of the distribution map of surface albedo in this area in early summer, at 1649 LST on 20 November 1990. Compared to Fig. 3, Lützow-Holm Bay is similarly perfectly covered with fast ice; the fast ice area extends slightly northward. The part of the Indian Ocean within this figure is also almost perfectly covered with pack ice except for the coastal polynya off the Riiser-Larsen Peninsula and the Ôtone Lead off Lützow-Holm Bay. The low albedo of less than 40 % is distributed in the open water in the form of polynyas

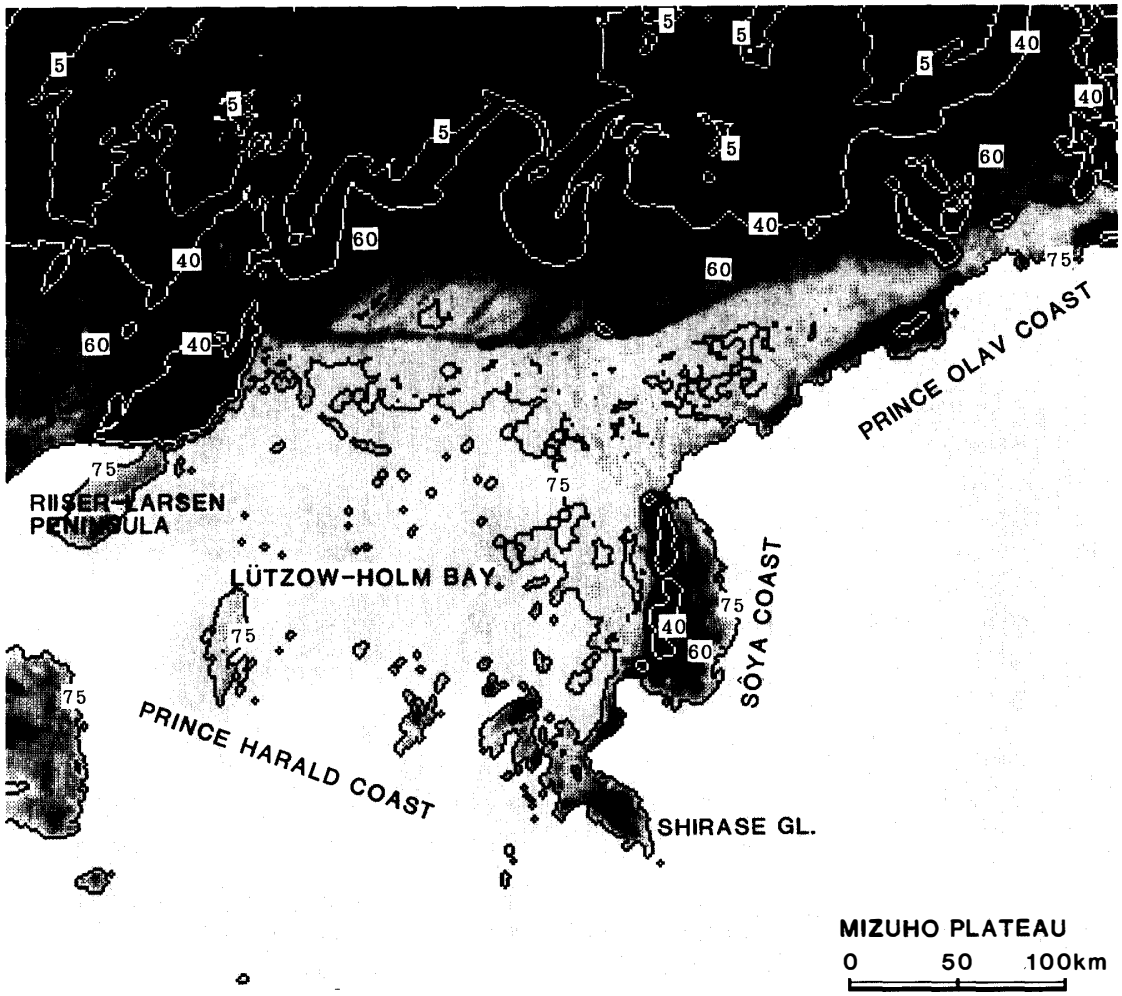

Fig. 3. The map of surface albedo in Lützow-Holm Bay and its neighborhood inferred with NOAA/AVHRR data for 1558 LST on March 12, 1990.

and leads. The albedo over the pack ice area is larger in the eastern part than in the western part due to the regional difference of sea ice concentration, and high albedos of more than 60 % occur here and there in the eastern part of the pack ice area. On the other hand, the albedo distribution pattern over fast ice and the Antarctic Continent is similar to Fig. 3. The magnitude, however, slightly increases, and low albedo extent of less than 75 % is reduced.

Figure 5 is a comparison of histograms between Figs. 3 and 4. Here, the solid line stands for 12 March 1990, and the dashed line for 20 November 1990. Each histogram has two almost common peaks, *i.e.* around 5 and 80 %. These correspond to, respectively, the open sea and fast ice. Although the albedo over pack ice ranges from 40 to 60 %, there is no obvious, corresponding peak in the histogram.

Among 16 cases analyzed by the present study, the distribution patterns of analyzed surface albedos are similar to each other, except for the seasonal variation of the pack ice area. However, since the number of samples is not enough and they are not sampled evenly in the whole year, it is impossible at

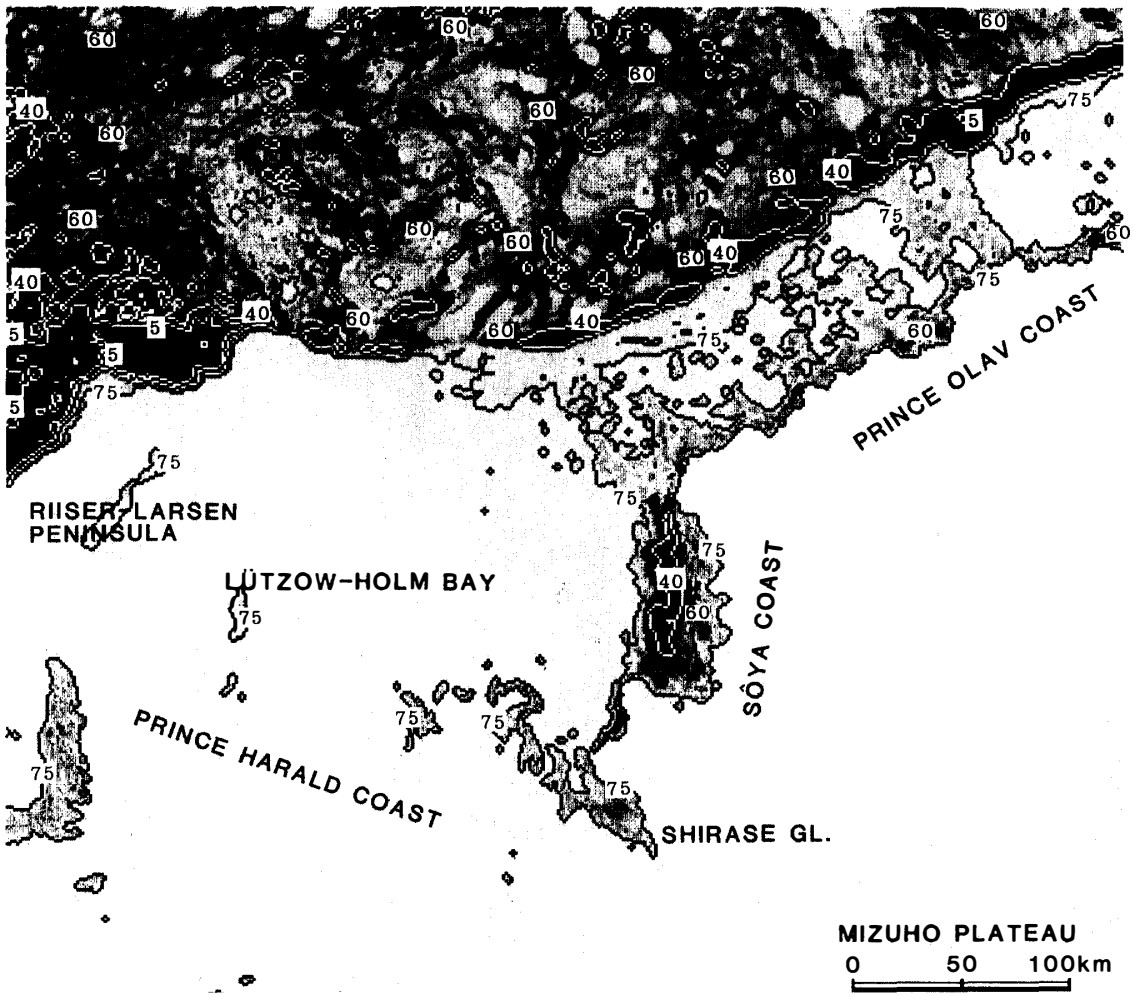

Fig. 4. The same as Fig. 3, except for 1649 LST on November 20, 1990.

present to discuss the annual variation in the surface albedo distribution over this area.

4. Comparison of Satellite-Inferred and Ground-Observed Albedos over the Sea Ice in Ongul Strait

Micrometeorological observations were done over the sea ice near Syowa Station from the end of March to the beginning of December in 1990. One of the purposes of the observations was to obtain ground truth data for surface albedo. Figure 6 shows the location of the observation point. This site was located about 2 km eastward off the station, almost in the center of Ongul Strait. The depth of the sea was 330 m; we always had sea ice more than 1 m thick during the whole year. Since the prevailing wind direction was NNE, the fetch of this site was large enough to observe the micrometeorological conditions. Not only the temperature and wind but also radiation were observed every 10 min at this site.

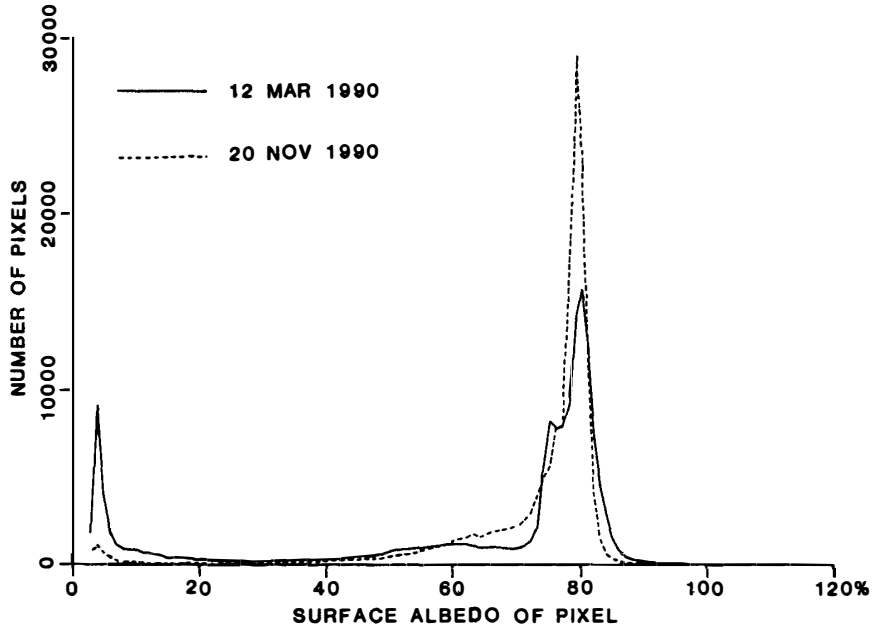

Fig. 5. Comparison of histograms of satellite-inferred surface albedos in Lützow-Holm Bay and its neighborhood between March 12 (solid line) and November 20 (dashed line) in 1990.

A summary of the micrometeorological observations is shown in Fig. 7. The bar in the upper part of Fig. 7 stands for the diurnal range of air temperature 4 m above the sea ice surface. The air temperature decreased gradually with day-to-day scatter since the beginning of the observations. The coldest season occurred at the end of August. After that the air temperature increased gradually with day-to-day scatter.

The day-to-day variations of the daily global solar radiation and albedo are shown in the lower part of Fig. 7. Solar radiation has a clear annual cycle; it decreased gradually from the beginning of the observations, and vanished at the end of May. The solar radiation appeared again at the middle of July, increased rapidly, and reached 35 MJ/m^2 per day in early summer. Although the surface albedo did not vary remarkably compared to solar radiation, there existed a clear annual cycle; the surface albedo over the sea ice with snow cover was higher in spring than in early summer, probably due to changes in snow density, liquid water content, and solar elevation (WARREN, 1982). In addition, there were remarkable day-to-day variations in both solar radiation and albedo, and both variations corresponded to each other; the surface albedo increased after a bad weather day when solar radiation decreased rapidly.

The solid square in the lower part in Fig. 7 stands for the satellite-inferred surface albedo of the pixel corresponding to the observation site. Although the observation site has snow cover with high albedo, there exists sea ice without snow cover to the eastward, and on the Ongul Islands which do not have snow cover to the west, which have very low albedo. As a result, the satellite-observed surface albedos vary rapidly pixel-to-pixel near the observation site. In addition,

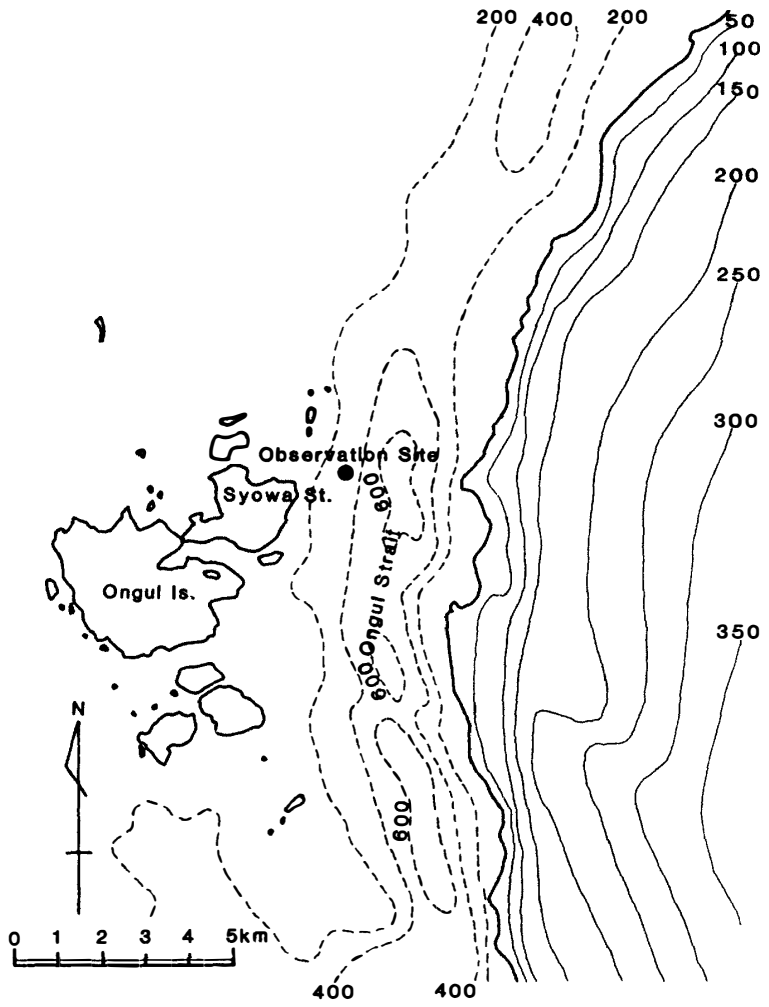

Fig. 6. The location of the observation site for surface albedo over the sea ice in Ongul Strait.

it is difficult to detect correctly the pixel including the observation site in the NOAA/AVHRR CCT data. Therefore, the present study plotted the highest inferred albedo among a few pixels in the northern part of Ongul Strait. As a result, we plotted 12 satellite-inferred albedos. As described above, ground-observed surface albedos were measured in the unfiltered spectral range, although the satellite-inferred surface albedos were obtained in the filtered spectral range. At first glance, however, both albedos agree well with each other.

Figure 8 shows a comparison of satellite-inferred and ground-observed surface albedos at the micrometeorological observation site in Ongul Strait. The abscissa is the daily mean ground-observed surface albedo, and the ordinate is the satellite-inferred surface albedo. The solid line in Fig. 8 stands for the best fit line, *i.e.* $y=x$. We note that almost all satellite-inferred albedos are lower than the corresponding ground-observed surface albedos. Letting the offset equal to zero, the following regression line is given:

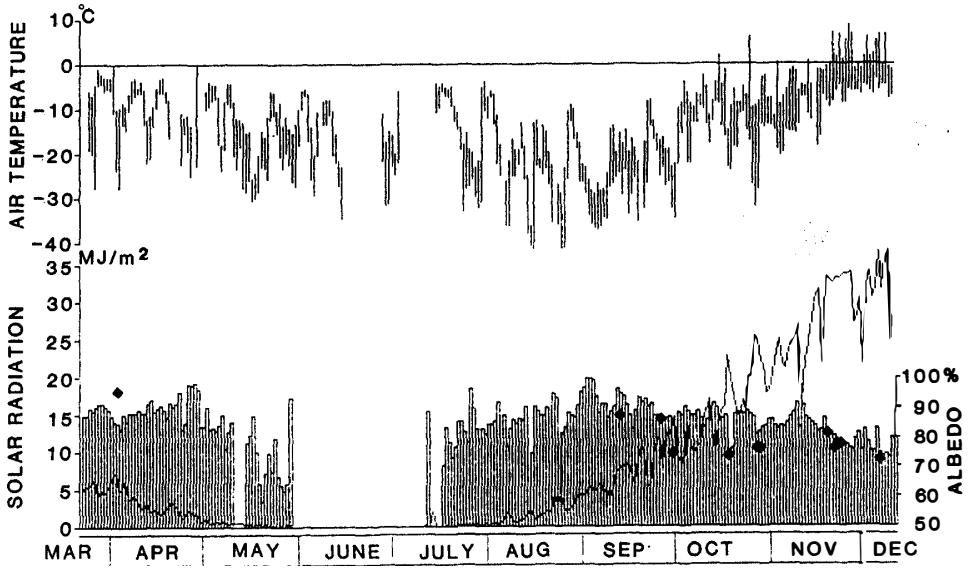

Fig. 7. A summary of micrometeorological observations over sea ice in Ongul Strait from the end of March to the beginning of December in 1990. The upper part is for the range of diurnal change of air temperature, and the lower part for the daily total of solar radiation and daily mean of surface albedo. The solid square is the satellite-inferred surface albedo of the pixel corresponding to this site.

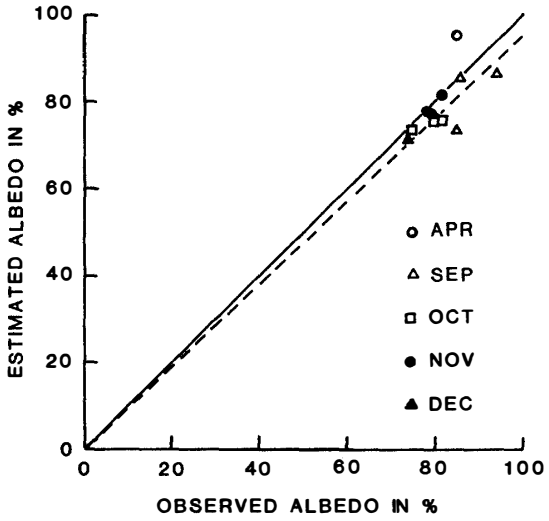

Fig. 8. Comparison between the ground-observed and satellite-inferred surface albedos over sea ice. The solid line is the best fit, and the dashed line for the regression line.

$$y = 0.963x, \tag{13}$$

where y and x are, respectively, satellite-inferred and ground-observed surface albedos. The correlation coefficient is 0.614. The dashed line stands for the above regression line. An explanation of this feature is that, although there are many uncertainties in deriving the point-to-point scatter, the surface albedo is correctly inferred by the present study, but that there exist systematic errors of about -4 %.

As mentioned above, the satellite-inferred surface albedo was derived from the filtered narrow band NOAA/AVHRR data, whereas the ground-observed

surface albedo was measured in the total solar spectral range. According to WISCOMBE and WARREN (1980), snow albedos are generally high in the near-ultraviolet and visible (0.3–0.7 μm) but start dropping off steeply with wavelength in the near-infrared between 0.8 and 1.5 μm and remain generally low for longer wavelengths. As the spectral regions of NOAA/AVHRR Channels 1 and 2 are mainly higher spectral snow albedo regions, the satellite-inferred surface albedo may be larger than the ground-observed surface albedo. To compare the filtered narrow band albedo in the spectral region of NOAA/AVHRR Channels 1 and 2 and the all wave albedo, both filtered and unfiltered albedos were calculated from the spectral snow albedos at a solar elevation of 30° (WISCOMBE and WARREN, 1980) weighted by the clear sky spectral flux at the solar elevation of 35° (CHOUDHURY and CHANG, 1981). As a result, the filtered narrow band albedos in the spectral regions of NOAA/AVHRR Channels 1 and 2 are 91.9, 84.9 and 77.9 %, respectively, for snow grain radii of 50 μm (new snow), 200 μm (2 days old snow) and 500 μm (older snow), whereas the corresponding broad band albedos are, respectively, 86.1, 79.5 and 74.1 %. In other words, the satellite-inferred surface albedo may be larger than the ground-observed surface albedo by about 5–7 %. This is contrary to the relationships of eq. (13).

Since the sensors of NOAA/AVHRR Channels 1 and 2 were calibrated at the ground before launching, it is possible for the sensitivity of sensors to decrease after that. Indeed, according to YAMANOUCHI (1990), it has been reported by C. JUSTUS that the sensitivity degradation of visible channel of NOAA11/AVHRR has been 5 % per one year after launching. At least, the above degradation counterbalances the excess of the filtered narrow band over unfiltered broad band albedos.

5. Concluding Remarks

The method proposed in the present study is a modification of the method of CHEN and OHRING (1984). The method used here is suitable for filtered narrow band NOAA/AVHRR measurements, whereas their original method is suitable for unfiltered broad band solar radiation. Therefore, the resulting albedo inferred here is also for the filtered spectral range. The conversion of filtered into unfiltered albedos is one of the most important recommendations.

As a result of a comparison with actual surface observations, it has been clear that, despite some systematic errors, the albedo estimated by the present study agrees well with the actually observed surface albedo. It is concluded that the albedo estimated here can be regarded as 96 % of the true, daily mean albedo. However, there remains significant scattering of the inferred albedo. Some such scattering may depend on the uncertainties of the method, such as an assumption of isotropy of upward radiation observed at a satellite, a detection of surface air temperature, vapor pressure, atmospheric pressure, total ozone amount and effective water vapor amount, and so on. The reconsideration and improvement of the above uncertainties is also an important recommendation.

The surface albedo distributions in Lützow-Holm Bay and its neighborhood have been analyzed for 16 days in 1990. As a result, it is clear that there exists a characteristic pattern of albedo distribution in Lützow-Holm Bay, and that the east extreme of this bay has a significantly low albedo. However, we could not obtain enough distribution maps to analyze the annual or inter-annual changes in surface albedo and its distribution. If we extend our analysis to all the data received during the period of ACR, these changes will also become clear.

Acknowledgments

The author wishes to express his sincere thanks to the members of the winter party of JARE-31 for their kind assistance both in receiving the satellite data at Syowa Station and in observing the micrometeorological conditions in Ongul Strait. He is also grateful to Dr. T. YAMANOUCHI, National Institute of Polar Research, for his useful discussion and comments, and to two anonymous referees for useful comments in revising this paper.

References

BRUTSAERT, W. (1975): On a derivable formula for long-wave radiation from clear skies. Water Resour. Res., **11**, 742–744.

CHEN, T. S. and OHRING, G. (1984): On the relationship between clear-sky planetary and surface albedos. J. Atmos. Sci., **41**, 156–158.

CHOUDHURY, B. J. and CHANG, A. T. C. (1981): The albedo of snow for partially cloudy skies. Boundary-Layer Meteorol., **20**, 371–389.

GRUBER, A. (1977): Determination of the earth-atmosphere radiation budget from NOAA satellite data. NOAA Tech. Rep., **NESS 76**, 28 p.

GRUBER, A., RUFF, I. and EARNEST, C. (1983): Determination of the planetary radiation budget from TIROS-N satellites. NOAA Tech. Rep., **NESDIS 3**, 12 p.

GURNEY, R. J. and HALL, D. K. (1983): Satellite-derived surface energy balance estimates in the Alaskan Sub-Arctic. J. Climate Appl. Meteorol., **22**, 115–125.

LACIS, A. A. and HANSEN, J. E. (1974): A parameterization for the absorption of solar radiation in the earth's atmosphere. J. Atmos. Sci., **31**, 118–133.

LIOU, K. N. and SASAMORI, T. (1975): On the transfer of solar radiation in aerosol atmospheres. J. Atmos. Sci., **32**, 2166–2177.

MEKLER, Y. and JOSEPH, J. H. (1983): Direct determination of surface albedos from satellite imagery. J. Climate Appl. Meteorol., **22**, 530–536.

NAKAGAWA, K. (1988): Estimation of the sky view-factor from a fish-eye lens image, considering the anisotropy of the downward longwave radiation. J. Meteorol. Soc. Jpn., **66**, 903–912.

OTTERMAN, J. and FRASER, R. S. (1976): Earth atmosphere system and surface reflectivities in regions from LANDSAT MSS measurements. Remote Sensing Environ., **5**, 247–266.

ROCKWOOD, A. A. and COX, S. K. (1978): Satellite inferred surface albedo over northwestern Africa. J. Atmos. Sci., **35**, 513–522.

THEKAEKARA, M. P. and DRUMMOND, A. J. (1971): Standard values for the solar constant and its spectral components. Nature (London), Phys. Sci., **229**, 6–9.

WARREN, S. G. (1982): Optical properties of snow. Rev. Geophys. Space Phys., **20**, 67–89.

WISCOMBE, W. J. and WARREN, S. G. (1980): A model for the Spectral albedo of snow. I: Pure snow. J. Atmos. Sci., **37**, 2712–2733.

YAMANOUCHI, T. (1990): Chikyû kibo kikô hendô ni okeru chihyômen hôsha shûshi (SRB) ni kansuru COSPAR/WCRP wâkushoppu shusseki hôkoku (Report of the COSPAR/WCRP workshop on surface radiation budget for climate and globalchange). Tenki, **37**, 116–118.

YAMANOUCHI, T., SUZUKI, K. and KAWAGUCHI, S. (1987): Detection of clouds in Antarctica from infrared multispectral data of AVHRR. J. Meteorol. Soc. Jpn., **65**, 949–962.

(*Received October 29, 1991; Revised manuscript received April 30, 1992*)